**Atmospheric
Chemistry
and Physics**

Gas-particle interactions above a Dutch heathland: I. Surface exchange fluxes of NH$_3$, SO$_2$, HNO$_3$ and HCl

E. Nemitz[1], M. A. Sutton[1], G. P. Wyers[2], and P. A. C. Jongejan[2]

[1]Atmospheric Sciences, Centre for Ecology and Hydrology (CEH), Edinburgh Research Station, Bush Estate, Penicuik, Midlothian, EH26 0QB, Scotland
[2]Energy Research Centre of the Netherlands (ECN), Postbus 1, 1755 Petten ZG, The Netherlands

Abstract. A field measurement campaign was carried out over a Dutch heathland to investigate the effect of gas-to-particle conversion and ammonium aerosol evaporation on surface/atmosphere fluxes of ammonia and related species. Continuous micrometeorological measurements of the surface exchange of NH$_3$, SO$_2$, HNO$_3$ and HCl were made and are analyzed here with regard to average fluxes, deposition velocities (V_d), canopy resistances (R_c) and canopy compensation point for NH$_3$. Gradients of SO$_2$, HNO$_3$ and HCl were measured with a novel wet-denuder system with online anion chromatography. Measurements of HNO$_3$ and HCl indicate an R_c of 100 to 200 s m^{-1} during warm daytime periods, probably at least partly due to non-zero acid partial pressures above NH$_4$NO$_3$ and NH$_4$Cl on the leaf surfaces. Although it is likely that this observation is exacerbated by the effect of the evaporation of airborne NH$_4^+$ on the gradient measurements, the findings nevertheless add to the growing evidence that HNO$_3$ and HCl are not always deposited at the maximum rate. Ammonia (NH$_3$) fluxes show mainly deposition, with some periods of significant daytime emission. The net exchange could be reproduced both with an R_c model (deposition fluxes only) using resistance parameterizations from former measurements, as well as with the canopy compensation point model, using parameterizations derived from the measurements. The apoplastic ratio of ammonium and hydrogen concentration (Γ_s=[NH$_4^+$]/[H$^+$]) of 1200 estimated from the measurements is large for semi-natural vegetation, but smaller than indicated by previous measurements at this site.

1 Introduction

The correct quantification of inputs of atmospheric pollutants such as oxidized nitrogen (NO$_y$), reduced nitrogen (NH$_x$) and sulphur compounds is an important prerequisite for the assessment of the impact of anthropogenic activities on natural and semi-natural ecosystems. The deposition of sulphur dioxide (SO$_2$), sulphate aerosols (SO$_4^{2-}$), nitric acid (HNO$_3$) and hydrochloric acid (HCl) have a direct acidifying effect, but even the deposition of the normally alkaline ammonia gas (NH$_3$) and neutral ammonium aerosol (NH$_4^+$) can cause acidification, depending on their fate within soil, water and plants (e.g. Binkley and Richter, 1987; Sutton and Fowler, 1993a). The additional eutrophying effect of the nitrogen (N) compounds (NH$_3$, NH$_4^+$ and HNO$_3$) may also be detrimental for many nitrogen limited ecosystems (e.g. Fangmeier et al., 1994).

Particularly in the Netherlands, with high concentrations of NH$_3$ and NH$_4^+$ arising from large livestock densities, inputs of atmospheric nitrogen have been held responsible for the poor state of heathland ecosystems (e.g. Bobbink et al., 1998): the additional N supply favours more nitrophyllous grass species which out-compete heather species characteristic of more oligotrophic conditions. It has also been suggested that atmospheric N deposition may raise the NH$_4^+$ concentration in the intercellular liquid in contact with the ambient air. This results in a high NH$_3$ emission potential (compensation point) of the heathland that partly limits the uptake of further NH$_3$ through stomata (Sutton et al., 1995a). However, large quantities of NH$_3$ and other reactive N can still be deposited to the leaf cuticles and may subsequently be washed off the leaves and taken up by the roots.

Measuring the deposition of reactive N is complicated through the dynamics of the chemical gas/aerosol equilibria of NH$_3$ and atmospheric acids with their associated NH$_4^+$ salts. Given the much faster exchange rate of gaseous species (NH$_3$, HNO$_3$, HCl and SO$_2$) if compared with their particulate counterparts (NH$_4^+$, NO$_3^-$, Cl$^-$ and SO$_4^{2-}$) (e.g. Duyzer, 1994), the phase partitioning between gas and aerosol can have a significant effect on local budgets and atmospheric transport distances. In addition, the formation (gas-to-particle conversion, gtpc) or evaporation of NH$_4^+$ aerosols (together gas-particle interconversion, gpic) can be

Correspondence to: E. Nemitz
(en@ceh.ac.uk)
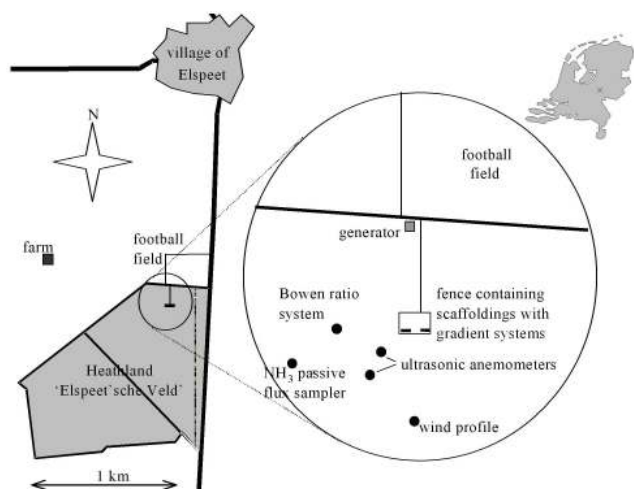
Fig. 1. Map of the Elspeet field site with instruments and the location within the Netherlands (inset).

fast enough to affect the micrometeorological techniques by which the surface exchange fluxes are estimated (Brost et al., 1988; Van Oss et al., 1998).

From 1995 to 1997 the "EXAMINE" project ("EXchange of AMmonia IN Europe") formed a first pan-European initiative to quantify the surface-exchange fluxes of NH$_3$ over a wide range of ecosystems and climates (Sutton et al., 1996). As part of EXAMINE, integrated international field campaigns were carried out to quantify exchange fluxes above a cereal crop in Germany ("Bellheim experiment", Meixner et al., 1996) and an oilseed rape field in southern Scotland ("North Berwick experiment", Sutton et al., 2000). During the latter campaign, surface exchange fluxes of HNO$_3$, HCl, SO$_2$ and aerosols were measured alongside the NH$_3$ exchange to study the effect of gas-particle interactions at a clean, maritime Scottish location (Nemitz et al., 2000b). It was found that, above the canopy, low acid concentrations led to a potential for evaporation of NH$_4$NO$_3$ and NH$_4$Cl. Due to low aerosol concentrations in general, however, timescales for the evaporation were estimated to be too slow for flux measurements and net exchange budgets to be affected by the process. This would be expected to be generally the case in clean environments. By contrast, within the canopy, the joint effect of daytime emission of NH$_3$ and HCl (the latter from unidentified sites in the canopy), gave rise to an occasional exceedance of the dissociation constant of NH$_4$Cl. Together with long residence-times within the canopy this may have provided a mechanism for aerosol production (Nemitz et al., 2000b).

A further integrated field campaign as part of EXAMINE was designed to study the surface-atmosphere exchange of NH$_3$ and to quantify the effects of gas-particle-interconversion in a more polluted environment than at North Berwick. These measurements took place at Elspeetsche Veld, a Dutch heathland three kilometres south of the village

of Elspeet near Appeldoorn, from 21 May to 13 June 1996, while measurements of the NH$_3$ surface exchange continued until the end of July (Hansen et al., 1999). At this location continental air masses, together with the high NH$_3$ concentrations typical for the Netherlands, were expected (a) to make gas-particle interactions more significant than at North Berwick and (b) to lead to concentrations well above the detection limit of the instruments. Elspeetsche Veld is a well studied field site, at which surface exchange fluxes were measured during several periods between 1989 and 1992 (Erisman and Duyzer, 1991; Bobbink et al., 1992; Erisman and Wyers, 1993; Erisman et al., 1994), although partly with less accurate instrumentation than available for this study. Previous measurements showed the NH$_3$ surface exchange at Elspeet to be bi-directional with deposition at night-time and emission fluxes of up to 550 ng m^{-2} s^{-1} during the day (Erisman and Wyers, 1993). Hence Elspeetsche Veld offered the prospect to study the effect of gpic during both strong emission and deposition of NH$_3$.

The present paper outlines the measurements and reports the concentrations of gaseous NH$_3$, HNO$_3$, HCl, HNO$_2$ and SO$_2$ measured with mainly denuder-based gradient systems. Surface exchange fluxes are quantified using the aerodynamic gradient technique assuming effects of gpic to be negligible. Furthermore, the NH$_3$ exchange is modelled using both an existing R_c resistance parameterization, obtained during a former campaign at the same site, and the canopy compensation point model of Sutton and Fowler (1993b) with parameterizations derived from the measurements presented here.

In order to simplify the analysis, the flux calculations are made here assuming the effects of gpic are negligible. However, parallel assessment of the aerosol-gas phase equilibrium at different heights in comparison with four other measurement sites suggests that there is significant potential for interaction with the dry deposition process Nemitz (1998). These interactions and their implications are therefore considered further in two companion papers: Firstly, Nemitz et al. (2004) report parallel eddy-covariance (EC) measurements of particle number fluxes as well as NH$_4^+$ aerosol fluxes by aerodynamic gradient method (AGM) from the Elspeet site, and apply these to assess the evidence of chemical interactions. Secondly, Nemitz and Sutton (2004) present a new numerical model developed to quantify the effects of gpic on the measured vertical gradients of NH$_3$/NH$_4^+$ and on the size spectra of NH$_4^+$ containing aerosols.

2 Methods

2.1 Field site description and synoptic meteorological situation

The vegetation of the Elspeetsche Veld (52°12′ N, 5°45′ E) is Genisto-Callunetum, a dry inland heath dominated by

Calluna vulgaris (L.)(Erisman and Wyers, 1993). The canopy was 9–10 year old canopy, with a height of 0.3–0.4 m, with patches of shorter rejuvenated heather (0.1–0.2 m), mainly in the SE wind sector. The measuring instruments were situated in the north-east part of the heathland, providing a uniform fetch of >200 m up to 1000 m in the wind sector 145° to 300° from N which covered the predominant SE and W wind directions (Fig. 1). Local NH_3 sources included several small farms located in the SW at distances of at least 3 km, and one farm as close as 1 km at WNW (Fig. 1).

The synoptic meteorology during the experiment can be divided into two periods: from 21 to 28 May the weather was dominated by the formation of an anticyclonic system with the centre over the British Isles. This period was characterized by light drizzle and moderate air temperatures (1 m height above the zero plane, d) reaching from 7–11°C at night to 14–16°C during daytime. Winds veered from SW on 21 to NNW on 25 May, while the surface windspeed at 1 m above d decreased from typically 4 m s^{-1} down to 1 m s^{-1}. On 26 May the wind increased again with the wind direction remaining unsteady between SW and N for the rest of this first period.

On 28 May a frontal system passed through, which was followed by a long warm period, dominated by a persistent high-pressure area stretching from Eastern Europe to the Iberian Peninsula. Until 4 June the overcast sky resulted in daytime temperatures of 15–27°C, whereas after 4 June temperatures increased from day to day reaching their maximum of above 34°C on 7 June (cf. Figs. 3 and 8 below). During clear nights temperatures dropped as low as 3°C, leading to significant dewfall during 5–11 June. At the same time the wind speed was more variable and showed a clear diurnal pattern with daytime values of 2–4 m s^{-1} and often dropped as low as 0.5 m s^{-1} during night. In the centre of the high pressure area, wind direction was unsteady, dominated by westerly winds but ranging from N through W to S.

2.2 Instrumentation

Concentration gradients of NH_3, HNO_3, HNO_2, HCl and SO_2 were principally measured by a range of continuous and automated wet-chemistry analyzers. Annular denuder inlets were used as a state-of-the-art method to discriminate between the gas and the aerosol phase with minimal interference. The rotating denuders consist of two concentric glass cylinders, that form a 1.3 mm wide annulus, through which a laminar air stream of about 28 l min^{-1} is drawn. Adsorption is provided by a $NaHSO_4$ solution for NH_3 and a K_2CO_3 solution for NH_3, HNO_3, HNO_2, HCl and SO_2. This solution is pumped through the denuder inlets in a counter flow and the solution from the different heights is fed sequentially to a conductivity cell for NH_4^+ analysis (AMANDA, ECN, Petten, Wyers et al., 1993) and to a Dionex anion chromatography (IC) system for the analysis of the other species (ECN, Petten)(Jongejan et al., 1997; Slanina et al., 2001). Previ-

ously, the denuder/IC system (DENIC) had only been used for concentration measurements of HNO_3, HCl, HNO_2 and SO_2 (Oms et al., 1996), but at Elspeet it was used for the first time in the field to obtain 2-point concentration gradients. The prototype employed here proved to be sensitive to the high ambient temperatures of >34°C temporarily observed at Elspeet, which led to occasional gaps in the data.

In addition, a 3-point gradient system of automated rotating batch denuders ("RBD", ECN, Petten)(Keuken et al., 1988) was used as a backup system. In these systems the collection solution, containing formic acid and NaOH, remained in the denuder tube for a 40-min sampling period, after which it was automatically pumped into test tubes for subsequent laboratory analysis. While all samples were analyzed for NH_4^+ on an Ammonia Flow Injection Analyzer (AMFIA, ECN, Petten, NL), financial restrictions meant that only a limited number of the batch denuder samples (7 days) could be analyzed for anions (NO_3^-, Cl^-, SO_4^{2-}) by anion chromatography using a DIONEX system. Further to these denuder systems, concentration gradients of the same species were also measured during 14 2-h runs using up to ten Ø 90-mm filter-packs (Sutton, 1990), containing a 1 μm PTFE particle pre-filter, a NaF impregnated filter for HCl and HNO_3 capture as well as a H_3PO_4 impregnated filter for NH_3 (Harrison and Kitto, 1990).

Accompanying the main measurements, a passive wind-vane sampling system for the cost-efficient measurement of long-term NH_3 fluxes was compared with the NH_3 fluxes derived from the AMANDA NH_3 gradient system for an extended period (23 May to 1 August). These results are reported elsewhere (Hansen et al., 1999). The main meteorological parameters and gas concentrations measured at Elspeet are listed in Table 1, together with the instrumentation and a reference to the techniques applied.

2.3 Micrometeorological theory

In the absence of fast response sensors for reactive and highly water-soluble gases such as NH_3 and HNO_3, (which would be necessary to measure fluxes by eddy-covariance), vertical concentration gradients were measured and the aerodynamic gradient technique was applied. According to Fick's law, the flux (F_χ) of a tracer (χ) is related to the vertical gradient of χ through the flux-gradient relationship for heat and inert tracers (K_H):

$$F_\chi = -K_H \left(\frac{z-d}{L} \right) \frac{\partial \chi}{\partial z} \qquad (1)$$

K_H is a function of the height (z) above d and atmospheric stability, parameterized as the Monin-Obukhov length (L), which is derived in this study from the sensible heat flux (H) and the friction velocity (u_*) measured by eddy-covariance using an ultrasonic anemometer (Garrat, 1992). In praxis, F_χ can be calculated from the logarithmic concentration profile

Table 1. Key parameters measured during the Elspeet campaign.

Approach applied[a]	Parameter (number of measurement heights)	Methodology	Averaging time /(method reference)	Manufacturer
(1) Gases				
AGM	NH_3 (3)	continuous AMANDA denuders with 3 inlets	6 min. cycle (3 inlets)	ECN, Petten, NL (Wyers et al., 1993)
AGM	NH_3 (4)	passive denuders (flux samplers)	5 days	(Hansen et al., 1999)
AGM	HNO_3, HCl, HNO_2, NH_3 (3)	automatic rotating batch denuder (RBD)	1 h cycle (40 min sampling)	(Keuken et al., 1988)
AGM	HNO_3, HCl, HNO_2, SO_2 (2)	continuous denuder/online anion chromatography (DENIC)	30 min (2 inlets)	(Oms et al., 1996)
AGM	NH_3 ($\leq$10)	filter-packs	1–3 h	(Harrison and Kitto, 1990)
AGM	SO_2 (3)	pulsed chemiluminescence analyzer	15 min cycle (2 inlets)	Thermo Environ. Inst., model 43s, Franklin, Mass., USA
(2) Micromet. measurements	mean humidity and temperature (1)	thermistor and capacitance probe	15 min	Rotronic Instr., Horley, Surrey, UK; Vaisala Ltd. Cambridge, UK
	net radiation, photosynthetically active radiation, wetness, precipitation	Bowen ratio system, wetness sensor, tipping bucket	15 min	Bowen ratio system, Campbell Scientific, Shepshed, UK
EC	instantaneous windspeed and temperature fluctuations (3)	ultrasonic anemometers	15 min	Solent Research 1012, Gill Instruments, Lymington, UK
EC	instantaneous water vapour fluctuations (1)	Krypton hygrometer (KH2O)	15 min	Campbell Scientific, Shepshed, UK
AGM	horizontal mean windspeed (6)	cup anemometers	15 min	Vector Instruments, Clywd, UK)
AGM	temperature and humidity gradients (2)	fine thermocouples and dewpoint meter	15 min	Bowen ratio system, Campbell Scientific, Shepshed, UK

[a] Key for flux measurement techniques: AGM – aerodynamic gradient method; EC – eddy covariance technique.

as (Garland, 1977; Sutton et al., 1992; Flechard and Fowler, 1998):

$$F_\chi = -u_* \kappa \frac{\partial \chi}{\partial \left\{ \ln(z-d) - \Psi_H \left[(z-d)/L \right] \right\}}, \quad (2)$$

where κ is the von Kármán constant (0.41). Ψ_H is the integrated stability correction function for heat and inert tracers, given as (Thom, 1975):

$$\Psi_H(\zeta) = -5.2 \left[(z-d)/L \right] \quad (3)$$

for stable conditions ($L > 0$) and

$$\Psi_H(\zeta) = 2\ln \left(\frac{1 + \left[1 - 16\left((z-d)/L \right) \right]^2}{2} \right) \quad (4)$$

for unstable conditions ($L < 0$).

2.4 Existing parameterizations of NH_3 surface/atmosphere exchange

2.4.1 The canopy resistance (R_c) modelling approach

A common way of parameterizing and predicting pollutant exchange with ecosystems is the resistance analogue. The flux is the result of a difference between the air concentration (χ_a) and the surface concentration (χ_0), as well as of the total atmospheric resistance (R_t).

$$F_t = -\frac{\chi_a - \chi_0}{R_t} \quad (5)$$

Two atmospheric resistances always contribute to R_t: the aerodynamic resistance (R_a) describes the transport through

the turbulent part of the atmosphere, and the sublayer resistance (R_b) describes the influence of the quasi laminar sublayer. Both resistances can be parameterized using micrometeorological parameters, and here the formulations of Garland (1977) are used. For many tracers the canopy acts as an efficient sink and therefore the surface concentration (χ_0) is assumed to be zero. In this case, the reciprocal resistance may be equated with the deposition velocity ($V_d=1/R_t$). In general, the exchange rate is limited by a further resistance at the surface itself, the canopy resistance (R_c):

$$F_c = -\frac{\chi_a}{R_t} = -\frac{\chi_a}{R_a + R_b + R_c} = -V_d\chi_a \tag{6}$$

The maximum value of the deposition velocity (V_{max}) is obtained where $R_c=0$ as

$$V_{max} = (R_a + R_b)^{-1}. \tag{7}$$

Earlier measurements at Elspeetsche Veld were used to derive parameterizations of R_c for SO_2 and NH_3 (Erisman et al., 1994; Jakobsen et al., 1997). The deposition of NH_3 to vegetation takes place via two main parallel pathways: exchange through the leaf stomata (described by the stomatal resistance, R_s) and adsorption to the leaf cuticles (described by the cuticular resistance, R_w) (Sutton and Fowler, 1993b). In the canopy resistance approach, R_c is calculated as the reciprocal sum of R_s and R_w (Fowler, 1978; Erisman et al., 1994):

$$R_c = \left(R_s^{-1}\,(NH_3) + R_w^{-1}\right)^{-1} \tag{8}$$

R_w can be considered as consisting of two parallel resistances for the deposition to leaves during high humidity (R_h or R_{ext}) and after rain (R_{rain}), respectively. Given the very infrequent rain events at Elspeet during the sampling period, R_w for NH_3 may be identified with R_{ext} as given by (Jakobsen et al., 1997):

$$R_w = 19\,257\exp(-0.094\,h) + 5, \tag{9}$$

where R_w is given in s m^{-1} and h is relative humidity in %. Erisman et al. (1994) furthermore suggested that $R_s(SO_2)$ at Elspeet be modelled according to Wesely (1989), using a minimum value of $R_{s,min}=250$ s m^{-1} for SO_2, which needs to be corrected for differences in molecular diffusivities (D_χ):

$$R_s\,(NH_3) = 250\frac{D_{SO_2}}{D_{NH_3}}\left(\frac{200}{St + 0.1}\right)^2\frac{400}{T\,(40 - T)}, \tag{10}$$

where St is the global radiation in W m^{-2} and T is the surface temperature in °C.

It has been pointed out that parameterizations obtained for Dutch conditions (NH_3/SO_2 ratios, temperature, humidity) may not be transferable to other countries (Erisman and Wyers, 1993). Indeed, problems have been encountered when these parameterizations were applied to less polluted environments such as a Scottish moorland site (Flechard and

Fowler, 1998). By contrast, Eqs. (8)–(10) should be re-applicable to Elspeet, apart from possible effects of changes in the pollution climate or vegetation status over the previous 5 years.

2.4.2 The canopy compensation point (χ_c) modelling approach

Clearly, the R_c approach adopted by Jakobsen et al. (1997) can only describe deposition and fails where NH_3 exchange is bi-directional, as in the case of agricultural high nitrogen ecosystems (Farquhar et al., 1980; Sutton et al., 1995b; Meixner et al., 1996). Periods of NH_3 emission were also observed during earlier measurements at Elspeet (Erisman and Wyers, 1993; Sutton et al., 1995b). Above such vegetation, emission is usually observed during warm daytime periods when high temperatures lead to elevated NH_3 concentrations in the substomatal cavities above the NH_4^+ dissolved in the apoplastic fluid, which is commonly referred to as the "stomatal compensation point" (χ_s)(Farquhar et al., 1980). The value of χ_s may be calculated from the ratio $\Gamma_s=[NH_4^+]/[H^+]$ of the apoplastic concentration of ammonium and hydrogen ions ($[H^+]=10^{-pH}$) as (Nemitz et al., 2000a):

$$\chi_s = \frac{161\,500}{T}\exp\left(-\frac{10\,380}{T}\right)\frac{[NH_4^+]}{[H^+]}$$
$$= \frac{161\,500}{T}\exp\left(-\frac{10\,380}{T}\right)\Gamma_s, \tag{11}$$

where all concentrations are given in mol l^{-1} at 1 atm and T is the temperature of the canopy in Kelvin. By contrast, during night, when stomata are closed, deposition to leaf surfaces (described by R_w) is the dominating pathway. The two competing processes of bi-directional stomatal exchange and cuticular adsorption are implemented in a single model by (Sutton and Fowler, 1993b). Central to the prediction of the net exchange flux is the canopy compensation point (χ_c), the average concentration at the canopy height:

$$\chi_c = \frac{\chi_s R_s^{-1} + \chi_a\,(R_a\,(z) + R_b)^{-1}}{(R_a\,(z) + R_b)^{-1} + R_s^{-1} + R_w^{-1}}, \tag{12}$$

from which F_t may be calculated from χ_c as

$$F_t = \frac{\chi_c - \chi_a}{R_a\,(z) + R_b}. \tag{13}$$

For dry daytime periods, $R_s(NH_3)$ may be derived from the stomatal resistance of water vapour transfer ($R_s(H_2O)$):

$$R_s\,(NH_3) = \frac{D_{H_2O}}{D_{NH_3}}R_s\,(H_2O)$$
$$= -\frac{D_{H_2O}}{D_{NH_3}}\frac{e_w\,(z_0') - e_{sat}\,(T\,(z_0'))}{E} \tag{14}$$

Water vapour pressure (e_w) and temperature (T) at the mean canopy height (z_0') can be calculated from the water vapour

Table 2. Summary of measured gas concentrations at Elspeet during the intensive measurement phase.

chemical species (instrument)	μ_A [μg m^{-3}]	μ_A [μeq m^{-3}]	σ_A [μg m^{-3}]	μ_M [μg m^{-3}]	σ_G [μg m^{-3}]	χ_{min} [μg m^{-3}]	χ_{max} [μg m^{-3}]	coverage [days]	meas. t [min]	N [#]
NH$_3$-N (AMANDA)[*)]	5.19 (6.07)	0.37 (0.43)	4.08 (4.46)	4.33 (5.05)	1.97 (1.72)	0.12 (0.40)	59.0 (59.0)	23 (15)	15 (15)	1881 (1157)
NH$_3$-N (RBD)	6.75	0.48	5.09	5.00	1.81	0.19	47.9	15	60	305
SO$_2$-S DENIC	1.69	0.11	1.45	1.33	1.44	0.16	8.69	21	30	284
SO$_2$-S (gas analyzer)	1.86	0.12	1.74	1.21	1.47	0.00	16.6	21	30	508
HNO$_3$-N (DENIC)	0.34	0.024	0.53	0.14	0.90	0.01	2.83	21	30	124
HONO-N (DENIC)	0.18	0.013	0.20	0.11	0.86	0.01	1.45	21	30	167
HCl-Cl (DENIC)	0.29	0.008	0.34	0.17	2.29	0.03	4.17	21	30	544

μ_A: arithmetic mean; σ_A: arithmetic standard deviation; μ_M: median; σ_G: geometric standard deviation; χ_{min}, χ_{max}: minimum and maximum concentration; meas. t: measurement time; N: number of observations. [*)] Values in brackets are for the same period as the rotating batch denuders (RBDs) to enable direct comparison of the results. Values are $\frac{1}{2}$ hour averages, except for RBD (40 min).
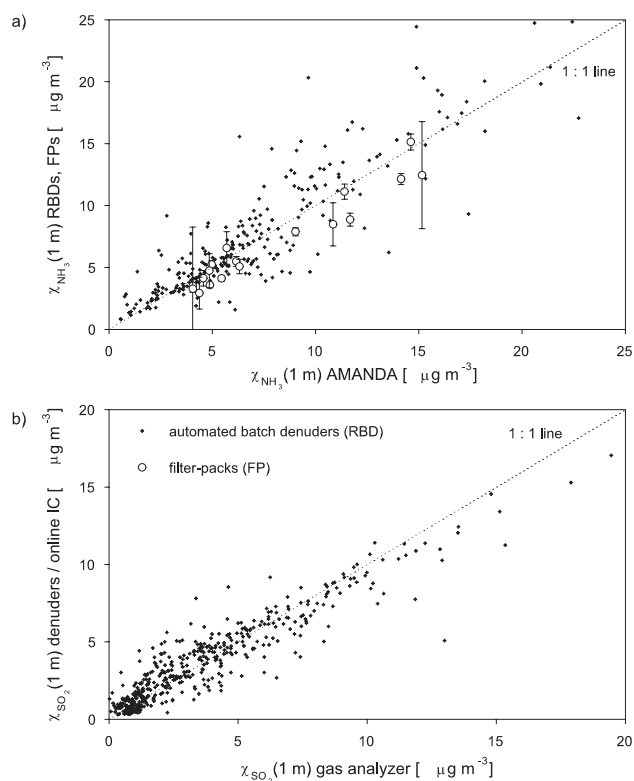
Fig. 2. Comparison of **(a)** NH$_3$ concentration measured with rotating batch denuders (RBD) and filter-packs (FP) against AMANDA reference system and **(b)** SO$_2$ concentration measured by the denuder system with online anion IC (DENIC) against a gas analyzer. Error bars show standard errors. Linear regression analysis yields: χ_{NH_3}(RBD)=1.03χ_{NH_3}(AMANDA)+0.34 (R^2=0.85), χ_{NH_3}(FP)=0.89χ_{NH_3}(AMANDA)−0.13 (R^2=0.93) and χ_{SO_2}(DENIC)=0.85 χ_{SO_2}(gas analyzer)+0.54 (R^2=0.88).

flux (E) and sensible heat flux (H), respectively (e.g. Nemitz, 1998). The water vapour flux (E) in g H$_2$O m^{-2} s^{-1}

was derived here from gradient measurements of the water vapour pressure with a Bowen ratio system (Campbell Scientific, Shepshed, UK). $e_{sat}(T(z_0'))$ is the saturated water vapour pressure at the mean T of the canopy ($T(z_0')$).

In the Netherlands, the χ_c-model has been successfully applied to NH$_3$ measurements over both forest and pasture (Sutton et al., 1995b; Plantaz et al., 1996; Wyers and Erisman, 1998), but this model has not yet been applied to Dutch heathland. However, from former measurements at Elspeet (Erisman and Wyers, 1993) an approximate compensation point may be estimated: for example, at 11:00 GMT on 14 September 1991 the flux switched from emission to deposition at an air concentrations (χ_a) of about 11 μg m^{-3} and a temperature (T) of 23°C, which corresponds to an emission potential (Γ_s) of 2500.

3 Measurement results

3.1 Concentrations

Ammonia concentrations were measured quasi-continuously by both the AMANDA system and RBD with additional support through several filter-pack runs, a comparison of which is shown in Fig. 2. Bearing in mind that the chemical analysis of the AMANDA concentrations was carried out online in the field, whereas batch denuder samples and filter extracts were analyzed in the lab by AMFIA, the agreement is reasonable. Compared with the other two methods, the filter-packs tended to underestimate the concentrations slightly. To assess the performance of the DENIC system, tested for the first time in the field, the SO$_2$ concentration was compared with a gas analyzer (Fig. 2b). Unfortunately, the gas analyzer proved to be noisy with a day-to-day zero drift of up to 2 μg m^{-3}. Considering this, the agreement is good, although the DENIC system underestimated the concentration on average by 12% compared with the gas analyzer. The concentrations of HNO$_3$ and HCl measured with the RBD systems were compared with the online IC system (data
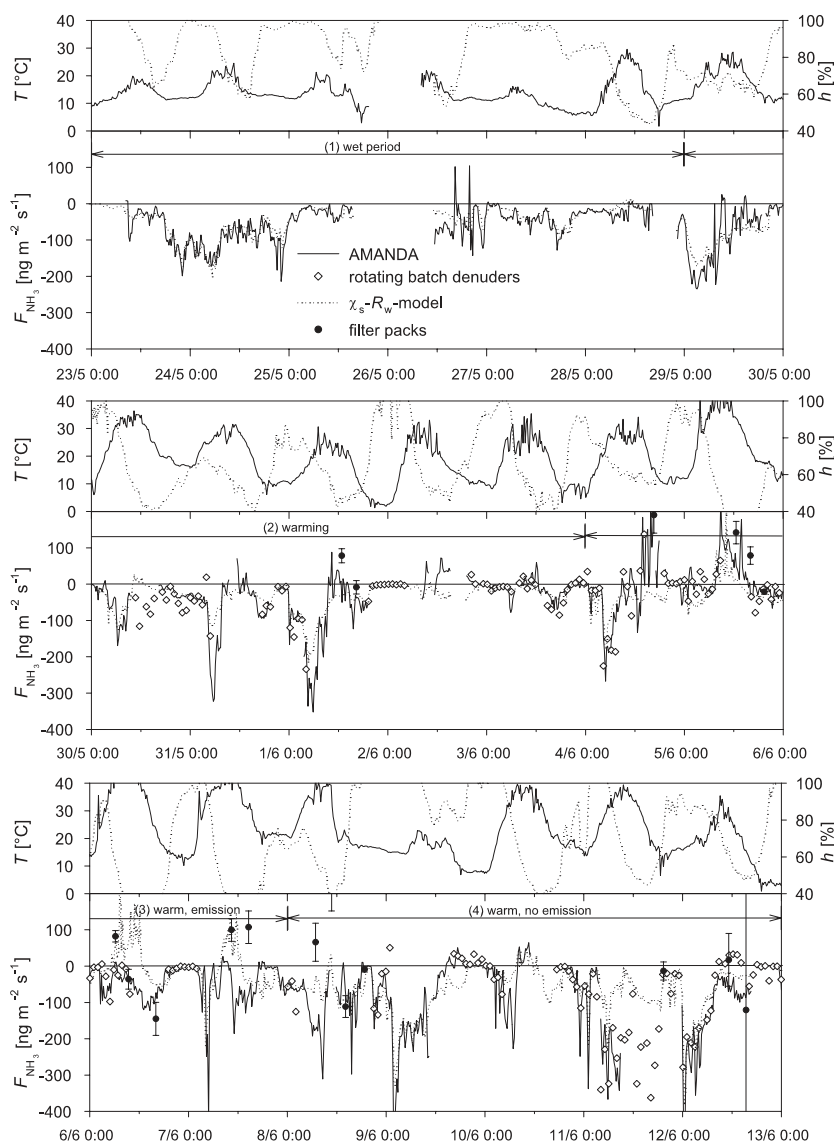
Fig. 3. The NH$_3$ flux at Elspeet measured with the AMANDA system, rotating batch denuders and filter-packs. Error bars are standard errors for 5–10 measurement heights. Also shown is the flux modelled with the χ_c-model calculating R_s and R_w according to Eqs. (15) and (17), respectively, with Γ_s=1200. The temperature at the canopy height ($T(z'_0)$) is shown as a solid line and the relative humidity at 1 m (h) as a dotted line.

not shown) and linear regression analysis gave the relationships χ_{HNO_3}(RBD)=1.04χ_{HNO_3}(DENIC)+0.59 (R^2=0.79) and χ_{HCl}(RBD)=1.32χ_{HCl}(DENIC)+0.22 (R^2=0.55), where concentrations are in μg m^{-3}.

From the gradient data, concentrations were interpolated to a height of $z-d$=1 m, and higher resolution data were block-averaged over 30 min. A summary of averages and standard deviations is given in Table 2.

3.2 Surface – atmosphere exchange fluxes

In this and the following sections the surface exchange fluxes of NH$_3$ and acidic gases are analyzed assuming the gradients

to be unaffected by chemical reactions. The validity of this assumption is discussed in Sect. 5.5 below and in more detail by Nemitz et al. (2004). The complete time-series of the NH$_3$ biosphere/atmosphere exchange flux is presented in Fig. 3, together with time-series of temperature (T) and relative humidity (h). According to T and h measurements the measurement period may be divided into four distinct measurement periods. The flux shows mainly deposition with the occasional appearance of daytime emissions (e.g. 4, 5 and 10 June 1996), mainly during period (3). The emissions on 4 and 5 June were associated with some of the highest canopy temperatures encountered so far in the growing season. Although the temperature increased even further during
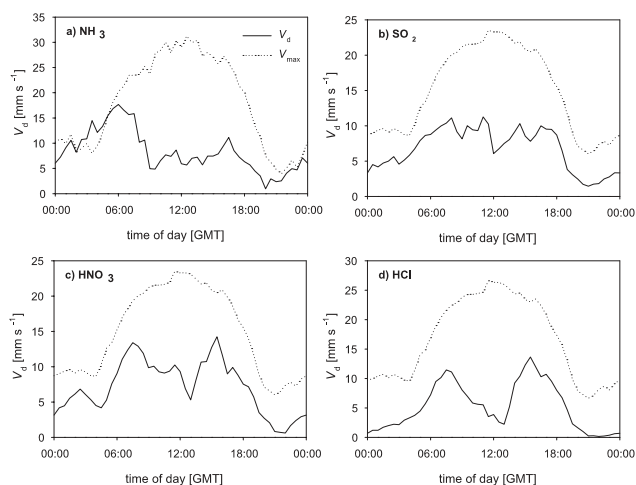
Fig. 4. Averaged diurnal cycles of the deposition velocities (V_d) as calculated from the AMANDA and DENIC gradients in comparison with V_{max}.

the subsequent two days the emission was not sustained. Possible reasons are discussed in Sect. 5.2 below.

During the intensive phase of the campaign presented here, the exchange flux ranged from -580 to $+240\,\mathrm{ng\,m^{-2}\,s^{-1}}$, with an arithmetic mean of $-55.1\,\mathrm{ng\,m^{-2}\,s^{-1}}$, a median of $-34.8\,\mathrm{ng\,m^{-2}\,s^{-1}}$ and a standard deviation of $78.3\,\mathrm{ng\,m^{-2}\,s^{-1}}$. By contrast, a considerably larger average of $-109\,\mathrm{ng\,m^{-2}\,s^{1}}$ was reported for the whole measurement period (Hansen et al., 1999). Despite stable stratification and reduced wind speeds at night, the deposition tended to be largest in the second half of the night, indicating a smaller R_c and higher NH_3 concentrations during night-time than during the day. This was also reflected in the averaged diurnal cycle of the deposition velocity for NH_3 (Fig. 4a), showing deposition at a rate close to V_{max} at night-time, as well as substantial deviation from V_{max} during the day.

The surface uptake resistance and/or the emission potential of the surface increased at 06:00 GMT and were largest around midday (09:00–16:00 GMT). The agreement in the fluxes measured with the AMANDA and RBD gradient is mostly impressive, although some periods of disagreement can be identified. By contrast, the FP gradients derive at times very different fluxes (e.g. 6–8 June).

A typical example of the surface exchange fluxes of HNO_3 and HCl is shown in Fig. 5, together with the comparison of V_d with V_{max} and R_c. During this period (3–4 June), both HNO_3 and HCl were found to be continuously deposited, but during daytime V_d calculated with the AGM for both gases was significantly less than permitted by turbulence. As R_c is calculated from the reciprocal V_d (Eq. 7), which is very large and uncertain during calm periods, values of R_c are only reliable during reasonably windy periods (i.e. $u_* > 0.1\,\mathrm{m\,s^{-1}}$; e.g. 4 June 04:00–20:00 GMT), where they show maximum values around midday of >200 and $100\,\mathrm{s\,m^{-1}}$ for HNO_3
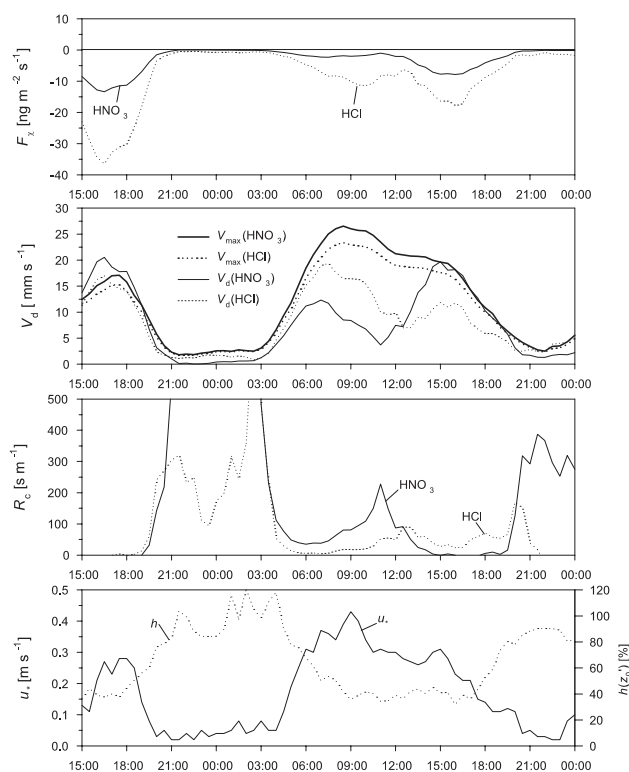
Fig. 5. Example diurnal cycle for 3–4 June 1996 of the **(a)** fluxes, **(b)** deposition velocities of HNO_3 and HCl in comparison with their maximum values and **(c)** R_c HNO_3 and HCl, **(d)** friction velocity (u_*) and relative humidity (h). Data represent 2.5 h running means of 30 min values, except for u_* and h (block-averaged for 30 min).

and HCl, respectively. From the averaged diurnal cycles of $V_d(HNO_3)$ and $V_d(HCl)$ (Fig. 4c, d) it may be seen that this is a general phenomenon for the whole period. Statistics of the deposition parameters V_d, V_{max}, R_c and $\chi(z'_0)$ are summarized in Table 3, separated for day and night-time as well as dry and wet periods as detected by the simple wetness grid sensor. The theoretical values of V_{max} are generally much smaller during night than during the day due to stable and calm conditions. Similarly, variability in V_d reflects not only changes in the uptake properties of the vegetation, but also changes in atmospheric turbulence. Thus, R_c and $\chi(z'_0)$ are generally more meaningful parameters for the description of the surface properties. Averaged values of R_c, however, should be treated with caution since negative values of R_c can be caused by two contrary conditions: overfast deposition ($V_d > V_{max}$) and emission. For NH_3, considerably larger values of R_c were derived for dry than for wet conditions. By contrast, deposition rates of HNO_3 and HCl appeared to be reduced during wet day time conditions. A more detailed analysis of the data revealed that the average for this category was biased by apparent deposition associated with drying leaf water layers in the morning hours on several days.

Table 3. Summary of deposition velocities and canopy resistances of gases at Elspeet for dry and wet conditions, as defined by the wetness sensor (day (04:00–19:00)/night-time (19:00–04:00).

			NH_3	SO_2	HNO_3	HCl
V_d [mm s^{-1}]	dry	min.	−27.7/−3.3	−32.6/−26.0	−30.1/−11.9	−21.9/−6.2
		max	31.1/40.2	49.6/28.7	42.4/26.2	66.9/32.5
		μ_A	6.0/6.9	9.3/4.8	10.9/3.4	13.3/2.5
		μ_M	7.2/4.8	8.4/2.8	11.5/2.2	11.7/1.7
	wet	min	−7.0/−2.5	−28.4/−31.2	−33.3/−13.1	−22.0/−14.1
		max	49.9/48.5	51.2/35.0	34.5/21.2	15.9/9.9
		μ_A	18.2/16.3	8.7/8.3	3.5/5.0	0.6/1.5
		μ_M	18.0/15.7	9.6/7.9	3.4/6.1	1.3/1.7
V_{max} [mm s^{-1}]	dry	min.	3.4/0.9	3.5/1.2	3.5/1.2	4.0/1.3
		max	44.9/29.8	31.0/24.5	31.0/24.5	35.2/27.5
		μ_A	25.8/8.0	19.5/6.5	19.5/6.5	21.9/7.2
		μ_M	19.5/5.9	19.9/4.6	19.9/4.6	22.3/5.1
	wet	min	4.0/1.9	5.8/3.7	5.8/3.7	6.2/3.9
		max	42.7/29.8	29.7/23.3	29.7/23.3	33.4/26.0
		μ_A	22.5/16.9	17.9/14.0	17.9/14.0	20.0/15.5
		μ_M	23.1/19.5	18.2/16.3	18.2/16.3	20.5/18.2
R_c [s m-1]	dry	μ_M	58/65	32.0/31.6	15.0/94.5	12.9/153
	wet	μ_M	9.6/8.5	−10.8/−13.9	21.2/38.6	46.7/183
$\chi(z_0')$ [μg m^{-3}]	dry	min	<0/<0	<0/<0	<0/<0	<0/<0
		max	18.7/15.2	21.1/11.2	5.3/7.3	1.7/3.4
		μ_A	4.9/1.3	0.82/0.28	0.44/0.73	0.04/0.26
		μ_M	4.8/1.9	1.45/0.34	0.42/0.34	0.10/0.10
	wet	min	<0/<0	<0/<0	<0/<0	<0/0.03
		max	10.3/10.8	16.9/6.8	4.9/4.5	1.9/1.4
		μ_A	0.59/1.1	0.19/0.60	0.51/0.28	0.21/0.21
		μ_M	0.75/0.70	0.27/0.04	0.17/0.12	0.15/0.11

min: minimum value; max: maximum value; μ_A: arithmetic mean; μ_M: median

For NH₃, $\chi(z_0')$ may be identified with the canopy compensation point (χ_c). This was largest during dry daytime conditions (4.8 μg m^{-3}) and much smaller during wet daytime conditions (0.6 μg m^{-3}). During wet conditions, a large fraction of stomatal emission would be recaptured by the leaf cuticle, which would provide efficient sinks. Wet canopies also coincide with cooler conditions and lower radiation, suppressing the stomatal emissions. The acidic gases were measured with prototype instrumentation at a lower time-resolution and at fewer heights than NH₃ and some more scatter in the data is therefore expected. On average, deposition velocities amount to only half of their theoretical maximum value. This is reflected by non-zero values of both R_c and $\chi(z_0')$.

4 Resistance modelling of the NH₃ vegetation/atmosphere exchange

The NH₃ flux was modelled with two different resistance models, using (a) the R_c model with parameterizations according to Eqs. (8) to (10), and (b) the χ_c-model according to Eqs. (11) to (13). In the following the parameterizations of the resistances R_w and R_s and Γ_s are derived for use in the χ_c-model.

4.1 Stomatal resistance

During stomatal opening, the mostly dry conditions allowed $R_s(NH_3)$ to be calculated from $R_s(H_2O)$, derived from the measured evapotranspiration (Eq. 12). $R_s(H_2O)$ was likely to be inaccurate either if turbulence was too low for R_a and R_b to be calculated accurately, or if evaporation of leaf-water layers contributed to E. Periods were therefore excluded if $R_a+R_b>200$ s m^{-1} or $h(z_0')>85\%$, and here R_{s,NH_3} was parameterized as a function of photosynthetically active radiation (PAR). In addition, $R_s(NH_3)$ was generally set to a night-time value of 4000 s m^{-1} (Van Hove et al., 1989) for PAR <20 W m^{-2}. By fitting a curve of the shape suggested by Sutton and Fowler (1993b) to R_s, the following overall
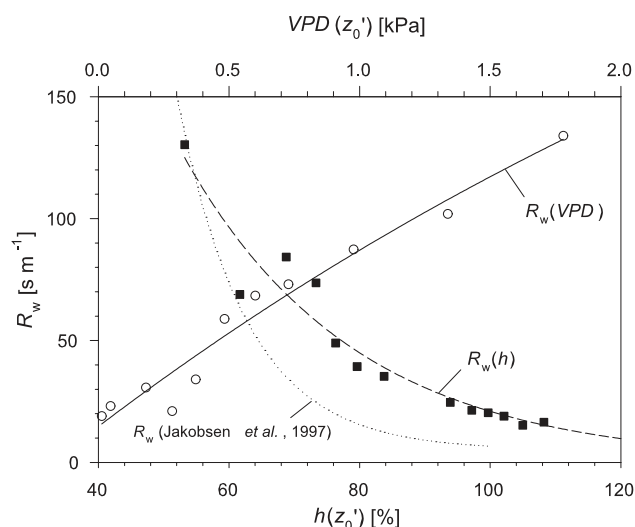
Fig. 6. The dependency of R_w for NH$_3$ on the surface values of relative humidity ($h(z_0')$)and vapour pressure deficit (VPD(z_0')). The full squares and open circles represent block-averaged values for 50 sequential 30-min values of R_w values, sorted for h and VPD, respectively. The dashed and the solid lines show the parameterizations of Eqs. (17) and (18), respectively, derived as fits to the measurements. The dotted line represents the parameterization of R_w (or R_{ext}) by Jakobsen et al. (1997), Eq. (9), for comparison.

parameterization was obtained:

$$R_s\,(NH_3) = \begin{cases} \frac{D_{H_2O}}{D_{NH_3}} R_s\,(H_2O)\,, & R_a + R_b\, <\, 200\,s\,m^{-1} \\ & \text{and}\quad h\left(z_0'\right) < 85\% \\ 4000, & PAR\, <\, 20\,Wm^{-2} \\ 100\left(1 + \frac{25}{2\times PAR}\right), & PAR\, \geq\, 20\,Wm^{-2} \end{cases}$$

(15)

For the temperatures encountered in this study, this parameterization agrees closely with the formulation by Erisman et al. (1994) of Eq. (10), suggesting that the stomatal conductance measured here is similar to the earlier measurements at this site.

4.2 Cuticular resistance

R_w was parameterized from periods selected for large R_s ($>1000\,s\,m^{-1}$) and excluding conditions of large $R_a + R_b (>500\,s\,m^{-1}$). During these periods, R_w can be approximated by the excess resistance of R_t compared with $R_a + R_b$ (e.g. Sutton et al., 1995b):

$$R_w \approx -\frac{\chi_a}{F_\chi} - (R_a + R_b)$$

(16)

The dependence of R_w on $h(z_0')$ and VPD(z_0') is shown in Fig. 6, together with parameterizations, derived from the data by least-square optimization:

$$R_w[s\,m^{-1}] = 11.4 + 178.7 \times (1 - \exp{(-0.546 \times VPD[kPa]))}$$ (17)

$$R_w\,[s\,m^{-1}] = 956.24 \times \exp{(-0.0382\ h\ [\%])}$$ (18)

and according to Eq. (9) for comparison. Equation (18) is numerically equivalent to the form of R_w applied by Sutton et al. (1995b) of $R_w = a\,\exp{((100-h)/b)}$, where $a = 21.0\,s\,m^{-1}$ and $b = 26.2$. During the present study R_w was larger and showed a weaker response to h than had previously been derived (Eq. 9) by Jackobsen et al. (1997).
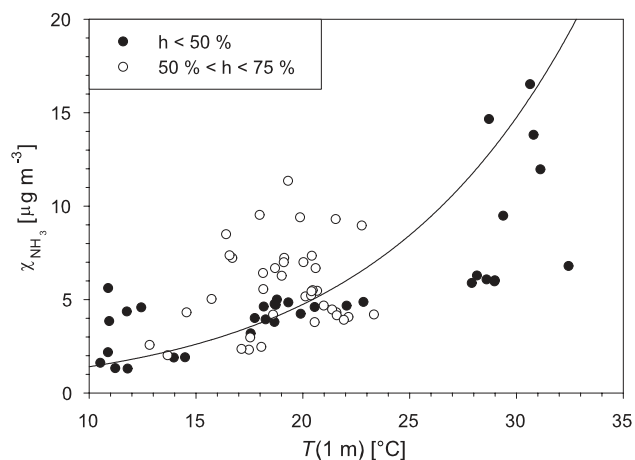
4.3 Emission and the stomatal compensation point

Ammonia emission from plant foliage can be the result either of a stomatal compensation point or desorption from leaf surfaces. Two observations suggest that stomatal exchange was probably the main reason for the emission observed: (i) emission occurred during long dry periods of up to 8 h (Fig. 3), while cuticular desorption is usually confined to the short periods of water layer evaporation (e.g. Sutton et al., 1998), and (ii) a high value of Γ_s was estimated from former measurements at Elspeet. However, the greatly reduced V_d for HNO$_3$ and HCl might also indicate that the sustained dissociation of previously deposited NH$_4$NO$_3$ and NH$_4$Cl salts provided sustained non-zero gas-phase concentration at the leaf surfaces, which could have led to the observation of prolonged emission at low concentrations and high leaf temperatures. Dynamic models, which have been described elsewhere, would be required to simulate cuticular desorption (Sutton et al., 1998; Flechard et al., 1999). For the application of the χ_c-model, the emission is therefore assumed in the present analysis to originate from leaf stomata.

Neglecting cuticular desorption, the emission potential of the foliage (Γ_s may be estimated from χ_a, observed during zero net fluxes: if stomatal exchange is dominant, as in the case for dry conditions (R_w large), a zero flux implies that $\chi_a = \chi_c = \chi_s$ (Eq. 13). Therefore, at low h, χ_s may be estimated from those values of χ_a at which the net flux changes from deposition to emission or vice versa (Spindler et al., 2001). Figure 7 shows these events as a function of T, together with the T-response curve of χ_s according to Eq. (11) for two values of Γ_s. A value of $\Gamma_s = 1200$ leads to a reasonable fit for $h < 50\%$, but for higher h, a distinct population of sign changes of the flux occur at larger air concentrations, which is probably caused by a contribution of cuticular desorption to the emission, which is most pronounced during the transition from a wet to a dry canopy.

4.4 Model results

The flux modelled with the χ_c-model and a value of $\Gamma_s = 1200$ is compared with the measured flux in Fig. 3. The model reproduces night-time deposition well, especially for the first half of the campaign, while emission is overestimated for the warm days 6 and 7 June. Daytime and night-time averages of the fluxes modelled with both the present parameterizations as well as the R_c model and the former parameterizations of Eqs. (8) to (10) are compared with the measurements in
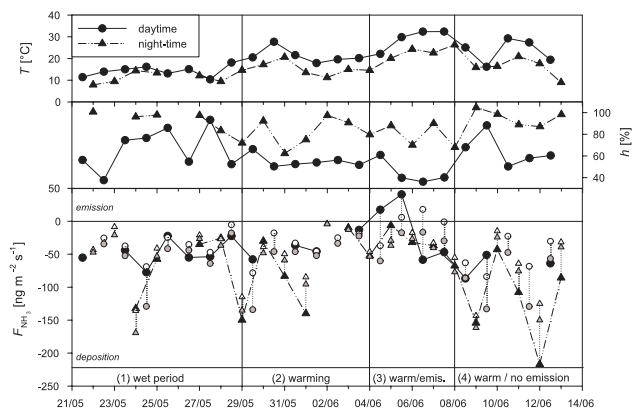
Fig. 7. The stomatal compensation point (χ_s) estimated from the NH$_3$ air concentration during individual events at which the flux changed sign as a function of temperature (T) for two ranges of relative humidities (h). Also shown are the T response curve calculated for a value of the apoplastic [NH$_4^+$]/[H$^+$] ratio (Γ_s) of 1200 according to Eq. (11).

Fig. 8. Daytime (circles) and night-time averages (triangles) of the NH$_3$ exchange flux modelled with (i) the χ_c-model (open symbols) and (ii) R_c-parameterization (grey symbols) according to Eqs. (8) to (10) in comparison with the measured values (black symbols).

Fig. 8. Table 4 shows measured and modelled day- and night-time fluxes for four distinct periods. The R_c model tends to overestimate daytime deposition, except for Period 3. By contrast, the canopy compensation point model underestimates net deposition during the wetter and cooler night-time conditions (Periods 2 and 4). This suggests that the R_w response to h may give rise to lower resistances during the day than at night, as found by Wyers and Erisman (1998), possibly due to the increased humidity around open stomata. During daytime the χ_c-model performs slightly better than the R_c-approach and predicts net emission on two days.

5   Discussion

5.1   Comparison of concentrations and fluxes and performance of the denuder/IC system

Bearing in mind the independent analysis techniques, the NH$_3$ concentration inter-comparison between AMANDA, RBDs and filter-packs showed good agreement (Fig. 2a; Table 2), comparable to that found during other comparisons (Harrison and Kitto, 1990). Whereas the AMANDA denuders were continuously flushed, some "outliers" in the batch denuder data may be the result of carry-over after episodes of high concentrations. Also, while the amount of collection solution was kept constant in the continuous denuders, strong variations in T and h led to evaporation of up to 80% of the collection solution from the RBDs, possibly resulting in periods of reduced capture efficiency. Despite problems with a noisy baseline of the SO$_2$ gas analyzer, the general functionality of the continuous denuder/IC combination (DENIC) was validated by the SO$_2$ inter-comparison (Fig. 2b). How-

ever, the HCl concentration detected by the RBDs was on average 25% larger than by the DENIC, which may reflect Cl$^-$ contamination of the RBD samples during transport and storage.

The AMANDA gradient system with online analysis is widely recognized to be a reference system for NH$_3$ flux measurements. By contrast, the much simpler RBDs are potentially affected by errors due to storage and operational checks in the field are virtually impossible. In this light, the agreement in the fluxes measured with AMANDA and RBD gradients is unexpectedly impressive, despite divergence on individual days.

5.2   Quantification and modelling of the NH$_3$ net exchange

From measurements at Elspeet carried out over the period 1990–1992, Erisman et al. (1994) estimated an average annual net throughfall flux of NH$_x$ (which is less than total NH$_x$ deposition due to canopy exchange processes) to be 52 ng N m^{-2} s^{-1} (16.5 kg N ha^{-1} yr^{-1}), with a substantial contribution of NH$_3$ dry deposition (41 ng N m^{-2} s^{-1}=13.0 kg N ha^{-1} yr^{-1}). This latter value agrees remarkably well with the averaged dry deposition of 45 ng N m^{-2} s^{-1} found during the intensive 3-week period of this study. However, the average dry deposition flux during the whole inter-comparison period detected by AMANDA and passive flux samplers was much larger, at 89 and 105 ng N m^{-2} s^{-1}, respectively (Hansen et al., 1999). While the passive flux samplers may therefore on average overestimate deposition slightly, the AMANDA values were filtered for $u > 1$ m s^{-1}, which removed small night-time fluxes and may have biased the overall average and could thus explain a small part of the discrepancy. However, the same filtering procedure applied to the intensive period raised the net deposition estimate only slightly (by 9%) to 49 ng N m^{-2} s^{-1}. Another possible explanation could be the

Table 4. Summary of the measured and modelled NH_3 fluxes (in $ng\,m^{-2}\,s^{-1}$), divided into day and night as well as 4 meteorologically distinct periods. Bold figures indicate values that deviate from the measured fluxes by more than 25%. Night-time is taken as 7:00–20:00 GMT.

	Period 1 21–29/05		Period 2 29/05–03/06		Period 3 04–07/06		Period 4 08–14/06		Mean	
	day	night	day	night	day	night	Day	night	day	night
measured flux	−50.2	−67.4	−16.6	−53.7	−36.6	−72.8	−63.4	−106.6	−39.5	−72.3
modelled flux (χ_c-model)	−42.6	−53.3	**−29.8**	**−37.5**	**−10.1**	−62.3	−52.7	**−60.9**	−34.7	**−51.9**
modelled flux (R_c-model)	**−67.0**	−66.8	**−43.8**	−43.7	−37.6	−76.4	**−93.7**	**−74.1**	**−59.8**	−63.4
$T(z_0')$ [°C]	15.0	12.2	21.5	15.8	29.9	22.3	23.1	16.0	20.8	15.8
h (1 m) [%]	66.4	74.1	54.3	82.2	46.1	83.2	64.2	93.2	59.4	81.1

typically wetter and more turbulent conditions over the extended period (not quantified), while air concentrations were similar.

Using parameterizations of R_s, R_w and χ_s derived from the field data, the χ_c-model of Sutton and Fowler (1993b) reproduces the measured net exchange flux of the first two weeks of the campaign well (Fig. 3), while during 4–8 June daytime emission is overestimated compared with measurements. This predicted large emission flux is a consequence of the high canopy temperatures (up to 40°C), together with the high emission potential (Γ_s=1200), which was found from estimates of the stomatal compensation point (Fig. 7), but which is also necessary to obtain the observed emission on 3, 5 and 10 June.

The measurements during the very warm period 4 to 8 June show considerable day-to-day variability, while similar values in χ_a, $T(z_0')$, h and S_t led to similar emissions predicted by the χ_c model for 5 to 8 June. Concentrations were somewhat larger during 6 and 7 June ($11\,\mu g\,m^{-3}$) as compared with 3 and 5 June ($6\,\mu g\,m^{-3}$), but the difference is insufficient to have suppressed emissions during 6 and 7 June efficiently. Equation (11) implies that χ_s doubles every 5 or 6°C, and the temperature effect should have more than compensated for the differences in air concentration. Since daytime R_s was inferred from the rate of measured evapotranspiration, the effects of drought closure would be accounted for in the NH_3 modelling and can therefore be ruled out as the reason for the overestimation.

It is possible that apoplastic $[NH_4^+]$ concentrations (e.g. Husted et al., 2000) were reduced during hot periods, for example due to temperature sensitive biochemical production/assimilation processes or as a result of the emission. An alternative explanation may lie in the determination of the leaf temperature that determines χ_s. Unpublished measurements over an agricultural grassland have shown that the micrometeorologically derived value of $T(z_0')$ may be considerably larger than the actual temperature of growing leaves (Integrated GRAMINAE Experiment, Pierre Cellier, pers. commun.). The most likely cause is the contribution to $T(z_0')$ by dry litter material and senescent leaves which heat up more

effectively than transpiring vegetation. Finally, there is convincing evidence that the flux measurements were affected by the evaporation of NH_4^+ aerosol both in the air, but also on the leaf surfaces (see Sect. 5.5). This effect would have led to an overestimate of Γ_s in Fig. 7. Aerosol evaporation would have been larger during the warmer second and third week of the campaign and could explain at least a part of the poorer agreement between measured and modelled NH_3 flux found for this period (Nemitz et al., 2004).

There is a clear trend in the comparative magnitudes of modelled and measured fluxes during the period 4 to 7 June: the model predicts emissions during 5 to 7 June, related to the canopy temperature, while the measurements indicate emissions on 4 and 5 June, which were not sustained during 6 and 7 June. This could be explained by the evaporation of previously deposited NH_4^+ salts on the leaf surfaces, which might have been completely volatilised by the end of 5 June. Emission events appear to occur at the first warm days after rain events (cf. also 10 June). Brief emission events have previously been observed when leaf water layers evaporate in the morning and these may be reproduced by dynamic models (Flechard et al., 1999). By contrast, sustained emission events covering two days, such as 4 and 5 June have so far been attributed to stomatal emission.

For the first two weeks of the campaign the average deposition predicted by the χ_c-model agreed within 10% with the measured average, while the overestimated daytime emission during 4–7 June led to a 23% underestimation in net deposition ($-42.7\,ng\,m^{-2}\,s^{-1}$) for the whole period. In contrast, the R_c parameterization of Erisman et al. (1994) and Jakobsen et al. (1997) underestimated the deposition during the first two weeks, but led to a more accurate estimate over the whole period, although some features of the exchange pattern, such as net emission on 2 days, were not reproduced (Fig. 3).

When the first measurements of NH_3 exchange over natural and semi-natural surfaces were made, it was expected that NH_3 would be deposited at rates approaching V_{max} (e.g. Sutton et al., 1993; Duyzer, 1994). The observation of large R_c values and even emission from unfertilized canopies

took researchers by surprise (Sutton et al., 1992; Erisman and Wyers, 1993). In particular, NH$_3$ emission from heathland at ambient concentrations of up to 5 μg m^{-3} has been taken as an indication that the input of atmospheric N can lift the N status of natural and semi-natural plant communities, thereby raising their Γ_s (Sutton et al., 1992, 1995a; Sutton and Fowler, 1993b). The value of Γ_s=1200 used in the model is smaller than derived from former measurements at Elspeetsche Veld, but much larger than found for other semi-natural surfaces in cleaner environments. For example, Flechard and Fowler (1998) derived Γ_s=132 for a Scottish moorland and a Γ_s between 50 and 130 may be inferred from NH$_3$ flux measurements at a Scottish upland site, dominated by Trichorphorum ceaspitosum and Calluna vulgaris (Milford et al., 2001). Similarly, Rattray and Sievering (2001) derived compensations points for alpine tundra vegetation in the Rocky Mountains of Colorado, which would be consistent with Γ_s≈16. A value of Γ_s≈500 was derived from laboratory measurements of the NH$_3$ exchange fluxes with commerically grown Calluna vulgaris plants (Schjoerring et al., 1998), and Γ_s values as low as 20 were found from gas fumigation experiments and direct bioassay analysis of Luzula sylvatica (woodrush)(Hill et al., 2001).

The increase in Γ_s due to long term atmospheric N deposition effectively restricts the uptake of further atmospheric NH$_3$ by stomata. The NH$_3$ deposition that a low-N semi-natural surface would receive from the air concentrations found at Elspeet may be simulated in a scenario using the present parameterizations of R_w and R_s together with a value of Γ_s=132. For such a canopy the χ_c-model predicts an average increase of the deposition flux of -8.0 ng m^{-2} s^{-1} (i.e. an additional input of 2.2 kg N ha^{-1} yr^{-1}). Hence the present NH$_3$ dry deposition to this site may have been suppressed by this amount as a feedback response to the high inputs of N over past decades. In terms of the within-canopy fluxes, the largest differences apply to the stomatal component flux: the model for present day conditions predicts a net stomatal emission of $+8.9$ ng m^{-2} s^{-1} (equivalent to $+2.3$ kg N ha^{-1} yr^{-1}), while that for a pristine heathland predicts a net stomatal uptake of -2.8 ng m^{-2} s^{-1} (equivalent to -0.7 kg N ha^{-1} yr^{-1}). However, the component modelled cuticular fluxes dominate the net flux, with values of -41.2 ng m^{-2} s^{-1} under present conditions, and -45.5 ng m^{-2} s^{-1} for the pristine heathland model estimate.

5.3 Biosphere-atmosphere exchange of SO$_2$ and NH$_3$-SO$_2$ co-deposition

The average annual sulphur loading at Elspeet had previously been estimated as 50.7 ng S m^{-2} s^{-1} (16.0 kg S ha^{-1} yr^{-1}) from throughfall measurements to which SO$_2$ dry deposition contributed with 35.5 ng S m^{-2} s^{-1} (11.2 kg S ha^{-1} yr^{-1}) (Erisman et al., 1994). At 18.4 ng S m^{-2} s^{-1} the average deposition flux measured with the DENIC was considerably lower, which is consistent with the lower average air con-

centrations during this study (3.4 compared with 6 μg m^{-3}). Although the figures reported by (Erisman et al., 1994) must be considered more reliable for yearly averages, Dutch SO$_2$ concentrations have indeed declined continuously since 1979 (e.g. Erisman and Bleeker, 1997).

It can be shown theoretically that NH$_3$ deposition fluxes to leaf cuticles are larger, if they are accompanied by SO$_2$ deposition and vice versa (co-deposition)(Flechard et al., 1999). This is due the neutralization reaction within leaf water layers. However, field investigations into this effect are difficult to interpret (Erisman and Wyers, 1993; Sutton et al., 1993). Flechard (1998) found that R_w(NH$_3$) at a clean Scottish moorland site was smaller the more SO$_2$ compared with NH$_3$ had been deposited to the canopy during the 24 h preceding the measurements. Nemitz et al. (2001) compiled various R_w parameterisations derived for a range of ecosystems and found a significant positive correlation with the annual average NH$_3$/SO$_2$ concentration ratio across these sites.

The cuticular resistance (R_w) for NH$_3$ derived in this study is larger than had been found at Elspeet during 1990–1992 (Fig. 6). This increase of R_w would therefore be consistent with a decrease in SO$_2$ deposition at this site. It should be noted, however, that the R_w paramaterization derived here may have been biased by the unrepresentatively warm conditions found during the intensive period of this study. This caveat is supported by the higher NH$_3$ deposition found during the extended period of this study, which could be caused by smaller values of R_w, but also by more turbulent conditions (not compared).

5.4 Biosphere-atmosphere exchange of HNO$_3$ and HCl

Due to their reactivity and high water-solubility, HNO$_3$ and HCl are generally thought to be perfectly absorbed by plant canopies (R_c=0; V_d=V_{max}). This hypothesis has been supported by a number of measurements (Huebert and Robert, 1985; Dollard et al., 1987; Meyers et al., 1989; Muller et al., 1993), during which no significant deviation of V_d from V_{max} was observed. A re-evaluation of the HNO$_3$ V_d measured by Dollard et al. (1987) and Harrison et al. (1989), however, revealed a correlation with the R_c of NH$_3$, which may reflect effects of gas-to-particle conversion (Sutton et al., 1993).

At Elspeet both HNO$_3$ and HCl were found to be continuously deposited. The diurnal variation in V_d of these gases closely followed that of NH$_3$ and showed values close to V_{max} at night, but considerable divergence from V_{max} between 06:00 and 20:00 GMT (Figs. 4 and 5). This could either be due to a measurement artefact caused by airborne gas-particle interconversion or may reflect a real surface uptake resistance of the sometimes extremely warm dry canopy.

The concept of perfect adsorption of HNO$_3$ and HCl has repeatedly been challenged: Huebert et al. (1988) observed HNO$_3$ emission, which, although it could be explained by airborne NH$_4^+$ evaporation (Brost et al., 1988), might nevertheless have represented real surface emission.

In addition, Neftel et al. (1996) reported emission gradients of HNO_3 above semi-natural grassland, which they explained by volatilization of NH_4NO_3 from warm leaf surfaces, while Zhang et al. (1995) made similar observations above a Dutch heathland. Strong evidence for HCl emission from an oilseed rape canopy, probably due to HNO_3 reaction with sea salt deposited to the leaf cuticle, was reported by during the North Berwick experiment (Nemitz et al., 2000b). And, finally, in fumigation experiments with 10 ppb HNO_3, Cadle et al. (1991) observed that the resistance for HNO_3 deposition to the cuticle increased by a factor of 15 within 16 h after the leaf surfaces had been washed.

There is therefore ample evidence for a non-zero canopy resistance and even emission of HNO_3 and HCl in certain situations. Considering the small vapour pressure over HNO_3 and HCl solutions (Clegg and Brimblecombe, 1986; Brimblecombe and Clegg, 1990), apoplastic concentrations of NO_3^- and Cl^- are unlikely to be sufficient to cause a significant compensation point. By contrast, it is quite plausible that a non-zero gas-phase concentration in equilibrium with NO_3^- and Cl^- particles on (warm) leaf cuticles may have been responsible for the observations. These particles could either have been previously dry-deposited or may have formed on the cuticle as a result of evaporation of rain, dew or microscopic water layers. Such a cuticular concentration (χ_d) of HNO_3 and HCl would obviously increase with increasing T and decreasing h.

5.5 Gas-particle interconversion

The same conditions that favour re-evaporation of HNO_3 and HCl from leaf cuticles would also result in the volatilization of airborne NH_4NO_3 and NH_4Cl. This can lead to a positive flux divergence of HNO_3 and HCl, consistent with the observation of $V_d < V_{max}$ (Brost et al., 1988). That evaporation of NH_4^+ exercised an important effect on flux measurements at Elspeet is supported by several independent observations. These issues are discussed in detail in the companion paper by Nemitz et al. (2004) and these include (i) large apparent deposition rates of NH_4^+ aerosol, (ii) partial gas pressure products below the value in equilibrium with the aerosol phase, especially near the canopy (Nemitz, 1998), (iii) apparent emission of very fine particles. The quantification of the effect of NH_4^+ evaporation on HNO_3 fluxes through numerical modelling in the companion paper of Nemitz and Sutton shows that the flux at the upper measurement height may underestimate the surface deposition by typically 5.5%. This figure was inferred for an example day with high HNO_3 concentrations and the divergence from thermodynamic equilibrium may have been underestimated. Hence, airborne NH_4^+ evaporation could contribute significantly to the observation of $V_d < V_{max}$ for HNO_3 and HCl but is very unlikely to be sufficient to account for all the deviation.

The Elspeet experiment had been designed as a complementary study to the North Berwick experiment. At

N. Berwick, under clean Scottish conditions, aerosol concentrations were much lower than at Elspeet. At both sites vapour concentrations were not in equilibrium with the aerosol phase. However, at N. Berwick aerosol evaporation was inhibited by large chemical time-scales and/or the absence of volatile aerosol components, and the impact on surface/atmosphere exchange fluxes was therefore negligible (Nemitz et al., 2000b).

6 Conclusions

Simultaneous measurements of the gradients of NH_3, HNO_3, HCl, and SO_2, were analyzed to infer surface exchange fluxes, net inputs and deposition velocities to a heathland site. The NH_3 fluxes were reproduced using an existing R_c parameterization, as well as a canopy compensation point (χ_c) model, with parameters derived from the field measurements. The same dataset has been applied elsewhere to investigate gas-aerosol phase equilibrium at this heathland and its potential interaction with dry deposition processes (Nemitz, 1998; Nemitz et al., 2004).

Ammonia exchange was found to be bi-directional with mainly deposition and occasional emission events during the day. The χ_c-model reproduced the bi-directional net NH_3 exchange flux reasonably well, although on some warm and sunny days daytime emission is overestimated. In the absence of direct measurements of the apoplastic ammonium/hydronium ratio ($\Gamma_s=[NH_4^+]/[H^+]$), it cannot be decided whether Γ_s was biochemically suppressed during these warm days, whether the micrometeorologically derived average canopy temperature was unrepresentative for the temperature of growing leaves or whether Γ_s was derived too large for these days. While the extended nature of the measured NH_3 emissions suggest stomatal emission as the cause, a contribution to the emission from evaporation of NH_4^+ salts on leaf surfaces cannot be excluded.

Although the R_c parameterization is methodically not able to account for periods of emission, it could still reproduce the measured flux fairly well, owing to often strong deposition caused by high NH_3 air concentrations and the relatively small percentage of emission events ($<15\%$ of the time). The value of $\Gamma_s=1200$ estimated here is an order of magnitude larger than those reported for other heathland and moorland ecosystems, which is likely due to a feedback from the high N deposition in the Netherlands on the Γ_s value. This maybe overestimated if NH_4^+ volatilisation contributed to the emission events. However, Γ_s is still smaller than inferred from former measurements at the same site in 1991/1992.

Direct measurements of the SO_2 dry deposition and higher cuticular resistance for NH_3, compared with measurements carried out in 1992, indicate a reduction of SO_2 inputs over the past few years. The averaged diurnal cycle of the deposition velocities of HNO_3 and HCl as derived by the unmodified aerodynamic gradient technique, using a new continuous

denuder-based gradient system with online analysis by ion chromatography, show surface uptake resistances (R_c) of up to 100–$200\,\mathrm{s\,m^{-1}}$ during the day. Flux divergence due to the evaporation of airborne NH$_4$NO$_3$ and NH$_4$Cl containing aerosol probably accounts for a fraction of the difference between V_d and V_{max}. However, the largest part of the discrepancy almost certainly reflects a non-zero R_c, possibly due to the acid gas partial pressure in equilibrium with NH$_4^+$ salts on leaf surfaces. This confirms the occurrence of a non-zero R_c for HNO$_3$ and HCl suggested in previous studies.

Edited by: M. Ammann

References

Binkley, D. and Richter, D.: Nutrient Cycles and H$^+$ Budgets of Forest Ecosystems, Advances in Ecological Research, 16, 1–51, 1987.

Bobbink, R., Heil, G. W., and Raessen, M.: Atmospheric Deposition and Canopy Exchange Processes in Heathland Ecosystems, Environmental Pollution, 75, 1, 29–37, 1992.

Bobbink, R., Hornung, M., and Roelofs, J. G. M.: The effects of air-borne nitrogen pollutants on species diversity in natural and semi-natural European vegetation, Journal of Ecology, 86, 5, 717–738, 1998.

Brimblecombe, P. and Clegg, S. L.: Equilibrium Partial Pressures of Strong Acids over Concentrated-Solutions, 3. The Temperature-Variation of HNO$_3$ Solubility, Atmospheric Environment Part a – General Topics, 24, 7, 1945–1955, 1990.

Brost, R. A., Delany, A. C., and Huebert, B. J.: Numerical Modeling of Concentrations and Fluxes of HNO$_3$, NH$_3$, and NH$_4$NO$_3$ near the Surface, J. Geophys. Res.-Atmospheres, 93, D6, 7137–7152, 1988.

Cadle, S. H., Marshall, J. D., and Mulawa, P. A.: A Laboratory Investigation of the Routes of HNO$_3$ Dry Deposition to Coniferous Seedlings, Environmental Pollution, 72, 4, 287–305, 1991.

Clegg, S. L. and Brimblecombe, P.: The Dissociation-Constant and Henry Law Constant of HCl in Aqueous-Solution, Atmos. Environ., 20, 12, 2483–2485, 1986.

Dollard, G. J., Atkins, D. H. F., Davies, T. J., and Healy, C.: Concentrations and Dry Deposition Velocities of Nitric-Acid, Nature, 326, 6112, 481–483, 1987.

Duyzer, J.: Dry Deposition of Ammonia and Ammonium Aerosols over Heathland, J. Geophys. Res.-Atmospheres, 99, D9, 18 757–18 763, 1994.

Erisman, J. W. and Bleeker, A.: Emission, concentration and deposition of acidifying substances, Acid atmospheric deposition and its effects on terrestrial ecosystems in The Netherlands, edited by Heij, G. J. and Erisman, J. W., Studies in Environmental Science, 69, 21–81, 1997.

Erisman, J. W. and Duyzer, J.: A Micrometeorological Investigation of Surface Exchange Parameters over Heathland, Boundary-Layer Meteorology, 57, 1–2, 115–128, 1991.

Erisman, J. W. and Wyers, G. P.: Continuous Measurements of Surface Exchange of SO$_2$ and NH$_3$ – Implications for Their Possible Interaction in the Deposition Process, Atmospheric Environment Part a – General Topics, 27, 13, 1937–1949, 1993.

Erisman, J. W., Vanelzakker, B. G., Mennen, M. G., Hogenkamp, J., Zwart, E., Vandenbeld, L., Romer, F. G., Bobbink, R., Heil, G., Raessen, M., Duyzer, J. H., Verhage, H., Wyers, G. P., Otjes, R. P., and Mols, J. J.: The Elspeetsche Veld Experiment on Surface Exchange of Trace Gases – Summary of Results, Atmos. Environ., 28, 3, 487–496, 1994.

Fangmeier, A., Hadwiger-Fangmeier, A., van der Eerden, L., and Jaeger, H. J.: Effects of atmospheric ammonia on vegetation – a review, Environmental Pollution, 86, 43–82, 1994.

Farquhar, G. D., Firth, P. M., Wetselaar, R., and Weir, B.: On the Gaseous Exchange of Ammonia between Leaves and the Environment – Determination of the Ammonia Compensation Point, Plant Physiology, 66, 4, 710–714, 1980.

Flechard, C. R.: Turbulent exchange of ammonia above vegetation. Ph. D. Thesis, University of Nottingham, Nottingham, UK, 1998.

Flechard, C. R. and Fowler, D.: Atmospheric ammonia at a moorland site, II: Long-term surface- atmosphere micrometeorological flux measurements, Quarterly Journal of the Royal Meteorological Society, 124, 547, 759–791, 1998.

Flechard, C. R., Fowler, D., Sutton, M. A., and Cape, J. N.: A dynamic chemical model of bi-directional ammonia exchange between semi-natural vegetation and the atmosphere, Quarterly Journal of the Royal Meteorological Society, 125, 559, 2611–2641, 1999.

Fowler, D.: Dry Deposition of SO$_2$ on Agricultural Crops, Atmos. Environ., 12, 1–3, 369–373, 1978.

Garland, J. A.: Dry Deposition of Sulfur-Dioxide to Land and Water Surfaces, Proceedings of the Royal Society of London Series a – Mathematical Physical and Engineering Sciences, 354, 1678, 245–268, 1977.

Garrat, J. R.: The atmospheric boundary layer, Cambridge University Press, Cambridge, 315, 1992.

Hansen, B., Wyers, G. P., Nornberg, P., Nemitz, E., and Sutton, M. A.: Intercalibration of a passive wind-vane flux sampler against a continuous-flow denuder for the measurements of atmospheric ammonia concentrations and surface exchange fluxes, Atmos. Environ., 33, 27, 4379–4388, 1999.

Harrison, R. M. and Kitto, A. M. N.: Field Intercomparison of Filter Pack and Denuder Sampling Methods for Reactive Gaseous and Particulate Pollutants, Atmospheric Environment Part a – General Topics, 24, 10, 2633–2640, 1990.

Harrison, R. M., Rapsomanikis, S., and Turnbull, A.: Land Surface Exchange in a Chemically-Reactive System – Surface Fluxes of HNO$_3$, HCl and NH$_3$, Atmos. Environ., 23, 8, 1795–1800, 1989.

Hill, P. W., Raven, J. A., Loubet, B., Fowler, D., and Sutton, M. A.: Comparison of gas exchange and bioassay determinations of the ammonia compensation point in Luzula sylvatica (Huds.) Gaud. Plant Physiology, 125, 1, 476–487, 2001.

Huebert, B. J. and Robert, C. H.: The Dry Deposition of Nitric-Acid

to Grass, J. Geophys. Res.-Atmospheres, 90, ND1, 2085–2090, 1985.

Huebert, B. J., Luke, W. T., Delany, A. C., and Brost, R. A.: Measurements of Concentrations and Dry Surface Fluxes of Atmospheric Nitrates in the Presence of Ammonia, J. Geophys. Res.-Atmospheres, 93, D6, 7127–7136, 1988.

Husted, S., Schjoerring, J. K., Nielsen, K. H., Nemitz, E., and Sutton, M. A.: Stomatal compensation points for ammonia in oilseed rape plants under field conditions, Agricultural and Forest Meteorology, 105, 4, 371–383, 2000.

Jakobsen, H. A., Jonson, J. E., and Berge, E.: The multi-layer Eulerian model: Model description and evaluation of transboundary fluxes of sulphur and nitrogen for one year, EMEP/MSC-W Report 2/97, EMEP/Meteorological Synthesizing Centre – West, The Norwegian Meteorological Institute, Oslo, 1997.

Jongejan, P. A. C., Bai, Y., Veltkamp, A. C., Wyers, G. P., and Slanina, J.: An automated field instrument for the determination of acidic gases in air, International Journal of Environmental Analytical Chemistry, 66, 4, 241–251, 1997.

Keuken, M. P., Schoonebeek, C. A. M., Vanwensveenlouter, A., and Slanina, J.: Simultaneous Sampling of NH_3, HNO_3, HCl, SO_2 and H_2O_2 in Ambient Air by a Wet Annular Denuder System, Atmos. Environ., 22, 11, 2541–2548, 1988.

Meixner, F. X., Wyers, G. P., and Neftel, A.: Bi-directional exchange of ammonia over cereals, Proceedings of Eurotrac '96, edited by Borrell, P. M., Borrell, P., Kelly, K., Cavitas, T., and Seiler, W., Computer Mechanics Publications, Southampton, Garmisch-Partenkirchen, 129–135, 1996.

Meyers, T. P., Huebert, B. J., and Hicks, B. B.: HNO_3 Deposition to a Deciduous Forest, Boundary-Layer Meteorology, 49, 4, 395–410, 1989.

Milford, C., Hargreaves, K. J., Sutton, M. A., Loubet, B., and Cellier, P.: Fluxes of NH_3 and CO_2 over upland moorland in the vicinity of agricultural land, J. Geophys. Res.-Atmospheres, 106, D20, 24 169–24 181, 2001.

Muller, H., Kramm, G., Meixner, F., Dollard, G. J., Fowler, D., and Possanzini, M.: Determination of HNO_3 Dry Deposition by Modified Bowen-Ratio and Aerodynamic Profile Techniques, Tellus Series B – Chemical and Physical Meteorology, 45, 4, 346–367, 1993.

Neftel, A., Blatter, A., Hesterberg, R., and Staffelbach, T.: Measurements of concentration gradients of HNO_2 and HNO_3 over a semi-natural ecosystem, Atmos. Environ., 30, 17, 3017–3025, 1996.

Nemitz, E.: Surface/atmosphere exchange of ammonia and chemically interacting species, Ph. D. Thesis, UMIST, Manchester, 1998.

Nemitz, E. and Sutton, M. A.: Gas-particle interactions above a Dutch heathland: III. Modelling the influence of the NH_3-HNO_3-NH_4NO_3 equilibrium on size-segregated particle fluxes, Atmos. Chem. Phys. Discuss., 4, 1567–1621, 2004.

Nemitz, E., Sutton, M. A., Schjoerring, J. K., Husted, S., and Wyers, G. P.: Resistance modelling of ammonia exchange over oilseed rape, Agricultural and Forest Meteorology, 105, 4, 405–425, 2000a.

Nemitz, E., Sutton, M. A., Wyers, G. P., Otjes, R. P., Schjoerring, J. K., Gallagher, M. W., Parrington, J., Fowler, D., and Choularton, T. W.: Surface/atmosphere exchange and chemical interaction of gases and aerosols over oilseed rape, Agricultural and Forest

Meteorology, 105, 4, 427–445, 2000b.

Nemitz, E., Milford, C., and Sutton, M. A.: A two-layer canopy compensation point model for describing bi-directional biosphere-atmosphere exchange of ammonia, Quarterly Journal of the Royal Meteorological Society, 127, 573, 815–833, 2001.

Nemitz, E., Sutton, M. A., Wyers, G. P., Otjes, R. P., Mennen, M. G., van Putten, E., Hellemond, J., and Gallagher, M. W.: Gas-particle interactions above a Dutch heathland: II. Concentrations and surface exchange fluxes of atmospheric particles, Atmos. Chem. Phys. Discuss., 4, 1519–1565, 2004.

Oms, M. T., Jongejan, P. A. C., Veltkamp, A. C., Wyers, G. P., and Slanina, J.: Continuous monitoring of atmospheric HCl, HNO_2, HNO_3, and SO_2, by wet-annular denuder air sampling with on-line chromatographic analysis, International Journal of Environmental Analytical Chemistry, 62, 3, 207–218, 1996.

Plantaz, M. A. H. G., Slanina, J., and Wyers, G. P.: Surface/atmosphere exchange of ammonia over grazed pasture, ECN-C-96-085, ECN, Petten, 1996.

Rattray, G. and Sievering, H.: Dry deposition of ammonia, nitric acid, ammonium, and nitrate to alpine tundra at Niwot Ridge, Colorado, Atmos. Environ., 35, 1105–1109, 2001.

Schjoerring, J. K., Husted, S., and Poulsen, M. M.: Soil-plant-atmosphere ammonia exchange associated with Calluna vulgaris and Deschampsia flexuosa, Atmos. Environ., 32, 507–512, 1998.

Slanina, J., ten Brink, H. M., Otjes, R. P., Even, A., Jongejan, P., Khlystov, A., Waijers-Ijpelaan, A., and Hu, M.: The continuous analysis of nitrate and ammonium in aerosols by the steam jet aerosol collector (SJAC): extension and validation of the methodology, Atmos. Environ., 35, 13, 2319–2330, 2001.

Spindler, G., Teichmann, U., and Sutton, M. A.: Ammonia dry deposition over grassland – micrometeorological flux-gradient measurements and bidirectional flux calculations using an inferential model, Quarterly Journal of the Royal Meteorological Society, 127, 573, 795–814, 2001.

Sutton, M. A.: The surface/atmosphere exchange of ammonia, Ph. D. Thesis, University of Edinburgh, Edinburgh, 194, 1990.

Sutton, M. A. and Fowler, D.: Estimating the relative contribution of SO_x, NO_y and NH_x inputs to effects of atmospheric deposition, edited by Hornung, M. and Skeffington, R. A., Critical loads: concepts and application, HMSO, London, Grange-over-Sands, 12–14 February 1992, 1993a.

Sutton, M. A. and Fowler, D.: A model for inferring bi-directional fluxes of ammonia over plant canopies, WMO Conference on the Measurement and Modelling of ATmopsheric Composition Changes including Pollution Transport, WMO/GAW, WMO, Geneva, CH, Sofia, Bulgaria, 4–8 October 1993, 179–182, 1993b.

Sutton, M. A., Moncrieff, J. B., and Fowler, D.: Deposition of Atmospheric Ammonia to Moorlands, Environmental Pollution, 75, 1, 15–24, 1992.

Sutton, M. A., Pitcairn, C. E. R., and Fowler, D.: The Exchange of Ammonia between the Atmosphere and Plant-Communities, Advances in Ecological Research, 24, 301–393, 1993.

Sutton, M. A., Fowler, D., Burkhardt, J. K., and Milford, C.: Vegetation atmosphere exchange of ammonia: Canopy cycling and the impacts of elevated nitrogen inputs, Water Air and Soil Pollution, 85, 4, 2057–2063, 1995a.

Sutton, M. A., Schjorring, J. K., and Wyers, G. P.: Plant Atmosphere Exchange of Ammonia, Philosophical Transactions of the

Royal Society of London Series a – Mathematical Physical and Engineering Sciences, 351, 1696, 261–276, 1995b.

Sutton, M. A., Nemitz, E., Fowler, D., Wyers, G. P., Otjes, R., San Jose, R., Moreno, J., Schjoerring, J. K., Husted, S., Meixner, F. X., Ammann, C., Neftel, A., and Gut, A.: The EXAMINE Project: exchange of atmospheric ammonia with European ecosystems, Proceedings of Eurotrac '96, edited by Borrell, P. M., Borrell, P., Kelly, K., Cavitas, T., and Seiler, W., Computer Mechanics Publications, Southampton, Garmisch-Partenkirchen, 155–161, 1996.

Sutton, M. A., Burkhardt, J. K., Guerin, D., Nemitz, E., and Fowler, D.: Development of resistance models to describe measurements of bi-directional ammonia surface-atmosphere exchange, Atmos. Environ., 32, 3, 473–480, 1998.

Sutton, M. A., Nemitz, E., Fowler, D., Wyers, G. P., Otjes, R. P., Schjoerring, J. K., Husted, S., Nielsen, K. H., San Jose, R., Moreno, J., Gallagher, M. W., and Gut, A.: Fluxes of ammonia over oilseed rape – Overview of the EXAMINE experiment, Agricultural and Forest Meteorology, 105, 4, 327–349, 2000.

Thom, A. S.: Momentum, mass and heat exchange, edited by Monteith, J. L., Vegetation and the atmosphere, Academic Press, Chichester, UK, 57–109, 1975.

Van Hove, L. W. A., Adema, E. H., Vredenberg, W. J., and Pieters, G. A.: A Study of the Adsorption of NH$_3$ and SO$_2$ on Leaf Surfaces, Atmos. Environ., 23, 7, 1479–1486, 1989.

Van Oss, R., Duyzer, J., and Wyers, P.: The influence of gas-to-particle conversion on measurements of ammonia exchange over forest, Atmos. Environ., 32, 3, 465–471, 1998.

Wesely, M. L.: Parameterization of Surface Resistances to Gaseous Dry Deposition in Regional-Scale Numerical-Models, Atmos. Environ., 23, 6, 1293–1304, 1989.

Wyers, G. P. and Erisman, J. W.: Ammonia exchange over coniferous forest, Atmos. Environ., 32, 3, 441–451, 1998.

Wyers, G. P., Oties, R. P., and Slanina, J.: A Continuous-Flow Denuder for the Measurement of Ambient Concentrations and Surface-Exchange Fluxes of Ammonia, Atmospheric Environment Part a – General Topics, 27, 13, 2085–2090, 1993.

Zhang, Y., ten Brink, H. M., Slanina, J., and Wyers, G. P.: The influence of ammonium nitrate equilibrium on the measurement of exchange fluxes of ammonia and nitric acid, edited by Heij, G. J. and Erisman, J. W., Acid Rain Research: Do we have enough Answers?, Elsevier Science B.V., 103–112, 1995.